MICROVASCULAR RESEARCH 34, 46–58 (1987)

Flow-Dependent Rheological Properties of Blood in Capillaries

T. W. SECOMB

Department of Physiology, University of Arizona, Tucson, Arizona 85724

Received March 4, 1986

Velocity-dependent flow of human red blood cells in capillaries with inside diameters of 4 to 8 μm is described theoretically. Cells are assumed to flow in single file, with axisymmetric shapes. Plasma flow in the gaps between cells and vessel walls is described by lubrication theory. The model takes into account the elastic properties of red cell membrane, including its responses to shear and bending. Cell shape is computed numerically as a function of tube diameter and cell velocity over the range 0.001 to 10 cm/sec. Relative apparent viscosity and dynamic hematocrit reduction (Fahraeus effect) are also computed. Since effects of interactions between cells are neglected, the Fahraeus effect is independent of hematocrit, while viscosity varies linearly with hematocrit. At moderate or high cell velocities, about 0.1 cm/sec or more, cell shapes and rheological parameters approach flow-independent limits. At lower velocities, cells broaden as a result of membrane shear and bending resistance and approach the walls more closely. Consequently, apparent viscosity increases with decreasing flow rate. Predicted values are in agreement with *in vitro* experimental determinations. Flow cessation is not predicted to occur in uniform tubes at positive driving pressures. Elastic deformational energies associated with red cell shapes are computed, leading to estimates of the pressure difference required to drive red cells past typical irregularities in capillary lumen cross sections. The hindrance to flow resulting from such structural irregularities represents a potential rheological mechanism for cessation of capillary flow at very low driving pressures.

INTRODUCTION

The rheological behavior of blood in microvessels is an important determinant both of overall blood flow through a tissue and of detailed flow distribution within the microvasculature of the tissue. Blood in bulk exhibits a viscosity which increases substantially at low flow rates (Dintenfass, 1962). However, the rheological properties of blood in microvessels differ markedly from those measured in bulk. For instance, the apparent viscosity of blood in microvessels is substantially lower than its bulk value (Fahraeus and Lindqvist, 1931) over a wide range of vessel diameters. The question therefore arises whether the rheological properties of blood in microvessels are also strongly dependent on flow rate. Since microvascular flow rates vary considerably in both normal and pathological conditions, such dependence may be expected to have important physiological consequences.

For example, flow-dependent rheological effects may play an important role in capillary recruitment in skeletal muscle. In resting muscle, half or less of the capillaries are typically observed to be flowing at a given moment. When oxygen

0026-2862/87 $3.00

demand increases, as during exercise, the number of capillaries with flow increases, while increased oxygen supply leads to a decrease in the number of capillaries with flow. The accepted mechanism for local modulation of total flow in capillary networks is the adjustment of arteriolar flow resistance through relaxation or constriction (Duling, 1978). If the resistances of capillaries were to remain constant in this process, one would expect all vessels in a capillary network fed by a single arteriole to respond proportionately to changes in the arteriolar flow. In particular, flow would cease virtually simultaneously in all capillaries when the single arteriole feeding them constricted fully. However, several studies have demonstrated a graded response in the fraction of flowing capillaries to changes in arteriolar diameter (Gorczynski *et al.*, 1978; Honig *et al.*, 1980; Lindbom *et al.*, 1980; Lindbom and Arfors, 1985). This implies that capillary flow resistances do not remain constant during such changes, and that the proportional change in resistance varies from capillary to capillary.

Several hypotheses have been proposed to account for this apparent individual modulation of capillary resistance (Lindbom and Arfors, 1985). Precapillary sphincters have been observed in some tissues (Nicoll and Webb, 1955), but have not been shown to be participate in flow regulation of skeletal muscle. Klitzman *et al.* (1982) proposed a "passive sphincter" mechanism, in which progressive contraction of arterioles leads to constriction of the entrances to daughter capillaries. However, this mechanism cannot readily account for the sequential cessation of flow in capillaries resulting from gradual reduction of arterial pressure observed by Lindbom and Arfors (1985). Therefore, it seems worthwhile to explore the hypothesis that rheological mechanisms are responsible, and that the apparent viscosity of blood in capillaries varies in a nonuniform manner during changes in arteriolar flow.

Since blood plasma has almost constant viscosity, nonuniform variations in apparent viscosity are most likely to result from mechanisms involving the formed elements in blood, especially the red and white blood cells. "Leukocyte plugging," in which white cells obstruct capillary flow, has long been observed in the microcirculation (Sandison, 1932; Bagge *et al.*, 1977). Under pathological conditions involving increased numbers of circulating white blood cells, the white cells may indeed be the principal factor determining flow distribution in a capillary network. In normal blood, white cells also participate in determining capillary flow patterns, but the population of white cells does not seem large enough to account fully for the observed patterns of flow cessation, since each capillary segment typically contains at most a few tens of red cells, and white cells are 1000 times less numerous. Flow-dependent rheological effects due to red cells in capillaries remain as a possible cause of local variations in capillary resistance. This last hypothesis is addressed in the present study.

Several previous experimental and theoretical studies have examined the flow dependence of apparent blood viscosity in capillaries. Lingard (1979) and Driessen *et al.* (1984) used mammalian red blood cells in glass tubes. Lee and Fung (1969) and Sutera *et al.* (1970) performed experiments with macroscopic model cells. The theoretical models of Lighthill (1968) and Fitz-Gerald (1969) were based on lubrication theory, while Zarda *et al.* (1977a) and Skalak and Tözeren (1980) used a finite element method and included a more detailed formulation of red

cell mechanics. The model of Secomb *et al.* (1986) combines this mechanical formulation with lubrication theory. All these studies demonstrate that apparent capillary blood viscosity increases with decreasing flow velocity. Their results are discussed in more detail below and by Secomb *et al.* (1986).

In the present study, theoretical methods developed by Secomb and Gross (1983) and Secomb *et al.* (1986) are used to model axisymmetric red cell deformation and flow and to predict rheological behavior of human blood in uniform cylindrical tubes from 4 to 8 μm in diameter, at flow rates of 0.001 cm/sec and above. The deformational energy associated with red cell deformation in such tubes is calculated, and this is used to estimate the pressure difference required to propel a red blood cell past cross-sectional irregularities such as exist in capillaries *in vivo*.

FORMULATION OF THE MODEL

The theoretical model has been described by Secomb *et al.* (1986) and Skalak *et al.* (1986). Here, the main underlying assumptions are stated and the method is summarized. The model applies to single-file flow of red blood cells along uniform cylindrical capillary tubes. The gap between each red cell and the tube is assumed to be small compared with the length of the cell. Also, the Reynolds number of capillary flow is so small that viscous effects dominate inertial effects in the plasma. This makes it possible to use lubrication theory, an approximation to the equations of fluid motion in which inertial forces are neglected and the hydrostatic pressure is assumed constant across the gap, although it varies along the gap. A further important assumption is that red cell shapes are axisymmetric. Actual red cell shapes in capillaries are not axisymmetric, although they approach axisymmetric shapes in narrow capillaries and at large cell velocities.

Because axisymmetry is assumed, all points on the cell move with the same velocity. Tank treading, involving continuous membrane deformation, occurs as a result of asymmetry in cell shape (Secomb and Skalak, 1982) and is absent in the present model. Consequently, the stresses in the membane depend on the elastic response of the cell membrane, and neither the internal viscosity of the cell nor the viscous component of the membrane's viscoelastic behavior enters the model. Since the elastic modulus of isotropic membrane dilation is relatively large (about 500 dyn/cm), it is assumed that the cell deforms in an area-conserving manner.

The elastic shear modulus of the membrane is much smaller, 4.2×10^{-3} dyn/cm (Chien *et al.*, 1978), and so the membrane shears readily. The resultant shear stress in the membrane is assumed to be governed by the constitutive relation proposed by Evans and Skalak (1980, p. 77). To apply this relation to an axisymmetric membrane shell, we suppose that $t_s(s)$ and $t_\phi(s)$ are the components of membrane tension, where the independent variable s is arc length measured from the nose of the cell, subscript s denotes components in a plane containing the axis, and subscript ϕ denotes azimuthal components (see Fig. 1). Then the components of tension are

$$t_s = t_m + t_d \quad \text{and} \quad t_\phi = t_m - t_d \tag{1}$$

where

$$t_d = \kappa(\lambda^2 - \lambda^{-2})/2. \tag{2}$$

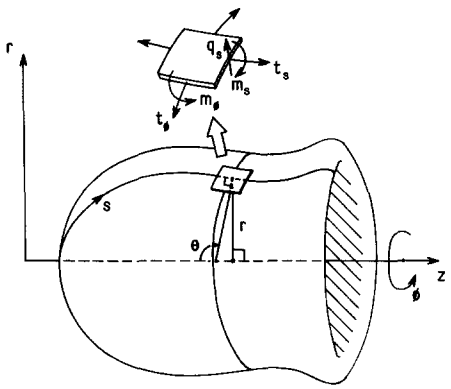

FIG. 1. Variables describing geometry and stress resultants in an axisymmetric cell.

Here $t_m(s)$ is the mean tension, κ is the shear modulus of the membrane, and $\lambda = ds/ds_0 = r_0/r$ is the extension of a membrane element in the s direction relative to the unstressed shape. Distance from the axis is denoted by $r(s)$, and the subscript 0 indicates the unstressed state. Because the membrane is treated as having infinite resistance to isotropic dilation, the mean tension $t_m(s)$ is indeterminate in the sense that it is not specified in terms of the membrane deformation.

In analyzing the effects of bending elasticity, we use the constitutive relation of Evans and Skalak (1980, p. 109), in which the bending moment is isotropic and proportional to the increase in total curvature of the surface. Therefore the components of bending moment, $m_s(s)$ and $m_\phi(s)$, satisfy

$$m_s = m_\phi = B[(k_s + k_\phi) - (k_s + k_\phi)_0] \tag{3}$$

where $k_s(s)$ and $k_\phi(s)$ are the principal radii of membrane curvature and B is the bending modulus, here assumed to be 1.8×10^{-12} dyn · cm (Evans, 1983). The two curvatures are related to the cell shape by

$$k_s = \frac{d\theta}{ds} \quad \text{and} \quad k_\phi = \frac{\sin\theta}{r} \tag{4}$$

where $\theta(s)$ is angle between the normal to the membrane and the axis.

For shear and bending stresses to be computed, the unstressed shape of the red blood cell membrane must be specified. The question of the existence and nature of an unstressed shape is not entirely settled (Fischer *et al.*, 1981). If axisymmetric deformed cell shapes are assumed, then an initially axisymmetric unstressed shape must also be assumed, coaxial with the vessel. Zarda *et al.* (1977a) assumed that the cell was unstressed in a biconcave disk configuration coaxial with vessel. Observations of red cells in narrow capillaries generally show, however, that the axis of the biconcave disc lies perpendicular to the vessel axis, leading to the so-called "crepe-suzette" shape in which the cell is folded over on itself. This presumbly leads to lower resistance than the coaxial orientation. However, this orientation of the unstressed shape is inconsistent with an axisymmetric model. Here, it is assumed instead that the membrane is unstressed in a spherical shape with the same surface area as the cell but with

increased volume. In this case, when the cell volume is set to its normal value, the calculated red cell shape is a biconcave disk with a somewhat smaller diameter and broader rim than is observed (cf. Zarda *et al.*, 1977b). Even so, the assumption of this unstressed configuration has the advantage that the membrane has no intrinsic preferred orientation with respect to the cell shape, so that the axisymmetric model may be applied in the case of a cell which enters "edgewise."

The membrane stresses must be in equilibrium with the external forces acting on the membrane. In this instance, the loading consists of the hydrostatic pressure difference $p(s)$ beteen the external and internal fluids and the viscous shear stress $\tau(s)$ due to the external fluid. For thin axisymmetric shells, the equations of mechanical equilibrium of normal stress, tangential stress, and bending moments are given by Timoshenko (1940):

$$\frac{1}{r}\frac{d(rq_s)}{ds} = p + k_s t_s + k_\phi t_\phi \tag{5}$$

$$\frac{1}{r}\frac{d(rt_s)}{ds} = t_\phi \cos\theta/r - k_s q_s - \tau \tag{6}$$

$$\frac{1}{r}\frac{d(rm_s)}{ds} = m_\phi \cos\theta/r + q_s \tag{7}$$

where $q_s(s)$ is membrane shear force per unit length.

According to the assumptions of lubrication theory, the hydrostatic pressure in the gap may be represented as $p(z)$ where z is the axial distance downstream of the front of the cell. From an analysis of the flow field, pressure gradient in the gap and shear stress on the cell membrane may be expressed in terms of cell radius $r(z)$, vessel radius a, suspending fluid viscosity μ, cell velocity u_0, and "leakback" q_0 per unit circumference. The leakback is the flow rate of suspending fluid relative to the cell. The resulting equations (Tözeren and Skalak, 1978; Secomb *et al.*, 1986) are

$$\frac{dp}{dz} = g(r) = \frac{16\mu}{a^2 - r^2}\left[u_0\left[\frac{a^2}{2} + \frac{a^2 - r^2}{4\ln(r/a)}\right] - a\,q_0\right] \times \left[a^2 + r^2 + \frac{a^2 - r^2}{\ln(r/a)}\right]^{-1} \tag{8}$$

$$\tau(r) = \frac{1}{4}g(r)\left[\frac{a^2 - r^2}{r\ln(r/a)} + 2r\right] - \frac{\mu u_0}{r\ln(r/a)}. \tag{9}$$

Two geometrical conditions complete the formulation:

$$\frac{dr}{ds} = \cos\theta \quad \text{and} \quad \frac{dz}{ds} = \sin\theta. \tag{10}$$

Then, from Eqs. (1)–(10), a system of six first-order nonlinear ordinary differential equations can be deduced, in which s is the independent variable and the dependent variables are r, θ, k_s, q_s, p, and t_s. The boundary conditions are that r, $\sin\theta$, and q_s vanish on the axis. Overall arc length (i.e., the length of the computational domain) and leakback are unknown parameters, but additional constraints come from the fact that surface area and volume are prescribed.

The solution procedure is described by Secomb *et al.* (1986), and is outlined here. To fix the length of the computational domain, a new independent variable is introduced, namely the angular distance from the axis at which a material element would lie if the cell were inflated to a sphere of the same surface area. Because the system of equations is singular on the axis, the numerical solution is obtained numerically over a slightly reduced domain excluding small regions near the axis, and matched to series solutions in those regions. For most parameter values of interest, the boundary value problem is ill-conditioned, i.e., when integrated starting at one boundary it is very sensitive to initial values. Because of this, a "multiple-shooting" method is used, in which the equations are integrated on a number (up to 66) of smaller subdomains. An iterative procedure is used to obtain matching between solutions on adjacent subdomains.

If the cell velocity is in the upper range of physiological values, a sharply curved cusplike shape is expected at the trailing edge of cell, leading to difficulties with the numerical method. For this case, an alternative approach was used, in which bending resistance was neglected. This leads to a simpler set of equations, which can be solved for higher cell velocities by methods similar to those already described. The resulting solutions for cell shape have a cusp of infinite curvature at the trailing edge, and the concave rear surface of the cell is approximated by a spherical segment. This approximate high-velocity analysis is justified by arguments of Secomb and Gross (1983), who reasoned that as cell velocity increases, membrane tension increases proportionately while bending stress remains bounded except possibly at the increasingly narrow cusp region. Therefore at high cell velocities, effects of membrane bending resistance become relatively small. Similarly, effects of membrane shear elasticity also become negligible in the high-velocity limit, leading to a configuration in which the dominant membrane stress over most of the cell surface is isotropic tension. Such a model, which predicts apparent viscosity and the Fahraeus effect to be independent of cell velocity, was proposed by Lin *et al.* (1973) and further developed by Secomb and Gross (1983). The present calculations approach the results of the isotropic tension model asymptotically at large cell velocities.

For each computed cell shape, the associated overall cell length l, pressure drop Δp across the cell, and leakback q_0 are also computed numerically. From these parameters, the Fahraeus effect and apparent viscosity may be predicted. The reduction in tube hematocrit due to the Fahraeus effect is related to the red cell velocity u_0 and the mean bulk velocity $\bar{u}$ by

$$H_T/H_D = \bar{u}/u_0 = 1 - 2q_0/au_0 \tag{11}$$

(Sutera *et al.*, 1970) where H_T is the tube hematocrit within the microvessel and H_D is the discharge hematocrit. To calculate the apparent viscosity μ_{app}, the pressure drop along a capillary segment containing a prescribed hematocrit is estimated by multiplying the computed pressure drop between the leading and the trailing edges of each cell (Δp) by the number of cells in the segment, and adding the pressure drop in the cell-free regions, which is assumed to be given by Poiseuille's law. In this approximation, effects of cell-to-cell interaction are neglected, and the resulting estimate of apparent viscosity depends linearly on

hematocrit:

$$\mu_{app} = \mu(1 + K_T H_T) \tag{12}$$

where

$$K_T = \frac{\pi a^2}{V}\left[\frac{\Delta p\, a^2}{8\mu(u_0 - 2q_0/a)} - l\right] \tag{13}$$

(Secomb *et al.*, 1986) and K_T is the apparent intrinsic viscosity.

RESULTS

Cell profiles computed by these methods are shown in Fig. 2 for a range of vessel diameters (Fig. 2a) and cell velocities (Fig. 2b). The corresponding three-dimensional cell shapes are generated by rotating these profiles around the axis of symmetry. In agreement with experimental observations and previous theoretical models, the computed shapes are rounded and convex in front (i.e., at the leading surface) and concave at the rear. When bending resistance is included, the sharp cusp at the trailing edge is replaced with a rim of finite curvature, as in the finite element results of Skalak and Tözeren (1980). This outwardly bulging rim is

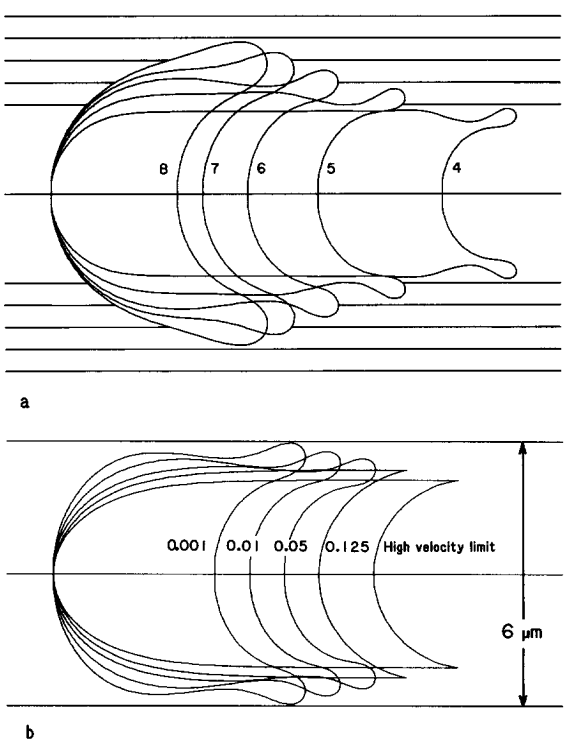

FIG. 2. Computed cell shapes. (a) Cell shapes at 0.01 cm/sec. Numerical values denote vessel diameters in micrometers. (b) Cell shapes in a 6-μm vessel. Numerical values denote velocities in centimeters/second. Calculations at 0.125 cm/sec and in the high-velocity limit neglect effects of bending resistance.

associated with the minimum gap width. The same behavior is shown in experimental observations of Bagge *et al.* (1980) and Gaehtgens *et al.* (1980).

In a vessel of given diameter, the cells widen as velocity decreases, as shown in Fig. 2b. The consequent reduction in leakback results in values of H_T/H_D nearer to unity, i.e., to a lessening of the Fahraeus effect, as shown in Fig. 3. The Fahraeus effect is also seen to increase substantially with increasing vessel diameter in this range. As cell velocity decreases, the increase in width is accompanied by a decrease in cell length, as indicated in Fig. 4. Cell length is also seen to depend markedly on capillary diameter, especially for diameters of 6 μm or less. In these figures, cell velocities beyond the normal physiological range have been included to show the asymptotic approach of the results to the high-velocity limit mentioned earlier.

As a consequence of these shape changes, apparent viscosity also varies with cell velocity. Predictions of apparent intrinsic viscosity K_T over a wide range of cell velocities are shown in Fig. 5. Over most of the range of velocities and diameters considered, the values are substantially lower than the value of K_T corresponding to the measured bulk viscosity of blood (K_T of about 7). Therefore, these results confirm a marked Fahraeus–Landqvist effect. The approach to the high-velocity limit is shown by the computations including shear but not bending elasticity. At cell velocities around 0.1 cm/sec, K_T exceeds its values in the high-velocity limit by between 5 and 60%, but remains relatively small. The calculations including bending elasticity predict a rapid increase in apparent viscosity at low velocities, 0.01 cm/sec and below. The finite element calculations of Skalak and Tözeren (1980) were based on similar assumptions, and also showed increasing viscosity at low velocities. The present calculations differ from those of Skalak and Tözeren (1980) in two main respects. First, values of K_T deduced from their results are substantially higher than those reported here for 7 and 8-μm capillaries, probably because of their different choice of unstressed red cell shape mentioned earlier. Second, their results were restricted to capillaries with diameters 7.45 μm or more, while the present approach using lubrication theory extends to vessel diameters as low as 4 μm.

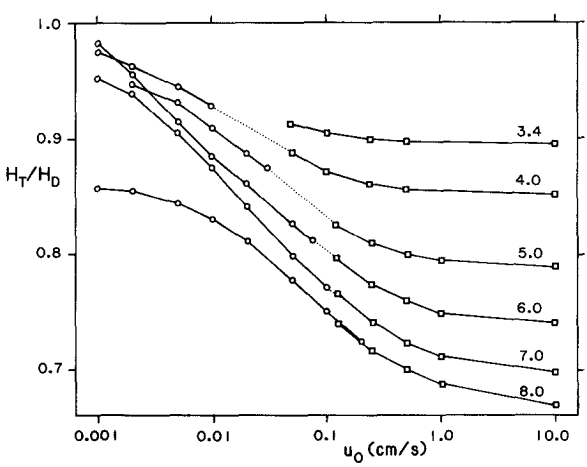

FIG. 3. Fahraeus effect as a function of cell velocity. Vessel diameter in micrometers is shown on each curve. Model including shear and bending effects: ○. Model neglecting bending resistance: □.

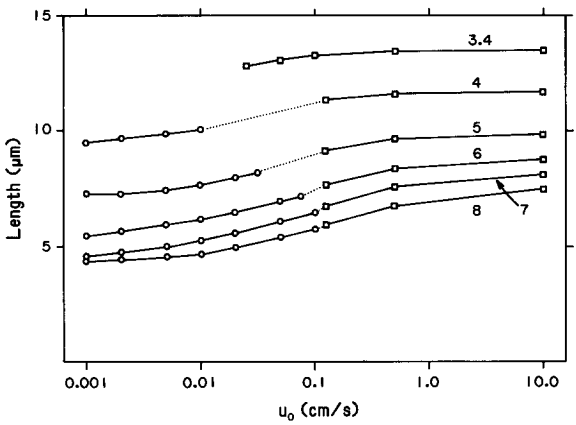

FIG. 4. Overall cell length as a function of cell velocity. Vessel diameter in micrometers on each curve. Model including shear and bending effects: ○. Model neglecting bending resistance: □.

Figure 5 indicates relatively weak dependence of apparent viscosity on vessel diameter between 4 and 7 μm. Similar behavior was found experimentally by Gaehtgens (1980) and theoretically in the high-velocity limit by Secomb and Gross (1983), and is seen here to apply at low velocities also. A rapid rise in apparent viscosity with decreasing diameter must occur near the critical diameter of about 3 μm (Secomb and Gross, 1983), but the present model could not be applied to such small-diameter vessels at low velocities, due to computational limitations.

Results of several experimental studies on flow dependence of apparent blood viscosity in capillaries are included in Fig. 5. Driessen *et al.* (1984) studied rat red blood cells flowing through 6.4-μm glass capillary tubes, while Lingard (1979) passed human red cell suspensions through arrays of capillaries of diameter 5.34

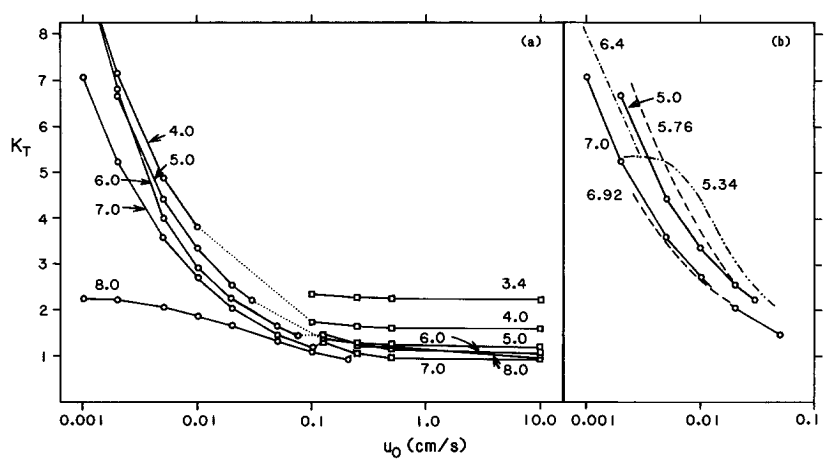

FIG. 5. Apparent viscosity as a function of cell velocity, expressed in terms of apparent intrinsic viscosity K_T. Vessel diameter in micrometers is shown on each curve. (a) Present results. Model including shear and bending effects: ○. Model neglecting bending resistance: □. (b) Comparison of present results in 5- and 7-μm vessels with experimental results: Lee and Fung (1969) (– –); Lingard (1979) (···–··); Driesen *et al.* (1984) (·–·).

μm. Lee and Fung (1969) used rubber model cells in their study. In plotting their data, we have rescaled vessel diameters according to cell dimensions, and velocities using a scaling based on the elastic moduli of the real and model membranes for uniaxial in-plane stress. This differs from the scaling used by Lee and Fung (1969), which was based on moduli for isotropic in-plane deformation. Sutera *et al.* (1970) also used flexible model cells. When rescaled by the same procedure, their results correspond to red cell velocities below the range considered here.

As Fig. 5 indicates, the results of the present model are in good agreement with available experimental data. A consistent trend of increasing viscosity with decreasing cell velocity is obtained. All the results for vessel diameters between 4 and 7 μm lie in a fairly narrow band. The discrepancies within this band between data from different sources are not surprising in view of the wide diversity of methods employed to obtain them. In vessels of diameter 8 μm, the red cell tends to a limiting shape at low velocities which is independent of flow forces, and so the apparent viscosity approaches an asymptotic value. Similar behavior in single-file flow is expected for vessels with diameters greater than 8 μm, whose cross sections are large enough to permit the passage of undeformed red cells.

Computations were made of the elastic deformational energy associated with the computed cell shapes, and the results are shown in Fig. 6 for a cell velocity of 10^{-2} cm/sec. From Eqs. (1)–(3), it may be shown that

$$\Delta E = \kappa(\lambda^2 + \lambda^{-2} - 2)/2 + B(\Delta k)^2/2$$

where ΔE is the energy per unit area and Δk is the change in total curvature. This quantity was integrated over the cell surface in each case. A rapid increase in deformational energy at diameters below 7 μm is apparent. Additional computations indicate a gradual increase in deformational energy with increasing cell velocity. Figure 6 also shows the increases in deformational energy associated with a decrease in vessel diameter of 1 μm at fixed cell velocity. These results provide an index of the ease with which a red cell can pass traverse an irregularity in the capillary lumen, such as a projecting nucleus. Ease of passage evidently decreases rapidly with decreasing capillary diameter.

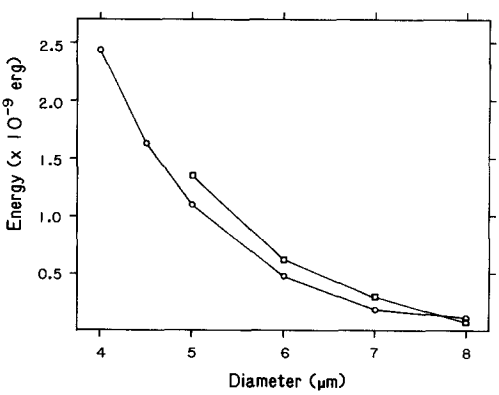

FIG. 6. Elastic deformational energy associated with cell shapes. Elastic energy of deformed state relative to assumed unstressed state: ○. Increase in elastic energy required for 1-μm decrease in vessel diameter: □.

DISCUSSION

In view of the rapid increase in apparent viscosity predicted at low velocities, it is natural to ask whether this model indicates a rheological mechanism for flow stoppage in capillaries when the driving pressure falls below some critical value. In case of such behavior, analogous to that resulting from a yield stress, one would expect apparent viscosity to vary as the inverse first power of flow velocity at low flow rates. However, the present results for flow in uniform cylindrical capillaries indicate that K_T varies approximately as $u_0^{-1/3}$, a weaker dependence. Consequently, red cells are predicted to continue to move when any pressure gradient, no matter how small, is present in the capillary. Of course, this conclusion is based on several assumptions invoked in developing the model, including uniformity of the vessel cross section.

The estimation of red cell deformational energies provides a means to examine possible effects of nonuniform cross sections on capillary flow at low velocities. As an example, we consider a capillary segment of length 100 μm and diameter 5 μm which contains four red blood cells, corresponding to a tube hematocrit of 0.18. If the cells are moving with a speed of 0.001 cm/sec, the apparent viscosity predicted by the present theory is about 0.03 dyn · sec/cm^2, yielding a pressure drop along the segment of approximately 40 dyn/cm^2. Now suppose that one cell encounters a local constriction of the capillary, and it undergoes a deformation to a new shape which corresponds to flow in a capillary of diameter 4 μm. The increase in elastic energy is then 1.3×10^{-9} erg. If this adjustment occurs as the cell travels a distance equal to its length, i.e., about 7.5 μm, then a pressure difference across the cell of at least 9 dyn/cm^2 is necessary to provide the elastic deformational energy. This represents nearly 25% of the available driving pressure. If all four cells encounter comparable obstacles simultaneously, and the available driving pressure remains constant, flow will cease. Therefore this order-of-magnitude calculation suggests that irregularities in vessel cross section can seriously interfere with flow at velocities of the order of 0.001 cm/sec in vessels of diameter 5 μm or less.

The above calculations are probably conservative in neglecting several factors tending to increase resistance to red cell motion. First, viscoelastic deformational resistance in the cell is neglected. Second, the lubricating plasma layer is likely to become very thin when a slowly moving cell encounters an obstacle, leading to increased viscous resistance. Third, low flow states are generally associated with a reduction in mean capillary pressure. Since capillaries are somewhat compliant, typical capillary diameters may then be reduced, tending to increase resistance to flow past localized vessel narrowings. In these calculations, luminal irregularities were assumed to be axisymmetric. In fact, obstructions are likely to be asymmetric in shape, and an equivalent axisymmetric constriction must be estimated. For instance, an endothelial nucleus projecting 1 μm into the lumen of a 5-μm vessel might have an effect similar to the 1-μm decrease in diameter postulated above. Although this very approximate analysis must be treated with caution, it seems reasonable to conclude that a pressure difference of the order of 10 dyn/cm^2/cell represents a lower bound on the minimum driving force required to sustain human red cell motion in narrow irregular capillaries.

In vivo cell shapes in capillaries are generally not axisymmetric, but it is not

known to what extent this affects the rheological properties. Secomb and Skalak (1982), using a two-dimensional model, predicted a reduced apparent viscosity for asymmetric cell shapes compared with corresponding symmetric shapes, associated with tank-treading motion. In single-file flow, however, observed tank-treading rates are quite low (Gaehtgens and Schmid-Schönbein, 1982), and so the rheological consequences are probably not very great.

In summary, a theoretical model for red cell motion in narrow capillaries, based on lubrication theory, axisymmetric red cell shapes, and a detailed simulation of red cell mechanical properties, predicts flow-dependent values of apparent viscosity in uniform tubes which agree well with available experimental data. According to this model, no critical minimum pressure or "yield stress" is required to maintain flow in a uniform vessel. However, irregularities in vessel cross section may lead to flow stoppage at very low driving pressures. This rheological mechanism may play a part in recruitment of capillaries with increasing flow rates in skeletal muscle.

ACKNOWLEDGMENT

This work was supported by NIH Grants HL17421 and HL34555.

REFERENCES

BAGGE, U., BRANEMARK, P.-I., KARLSSON, R., AND SKALAK, R. (1980). Three-dimensional observations of red blood cell deformation in capillaries. *Blood Cells* **6**, 231–237.

BAGGE, U., SKALAK, R., AND ATTEFORS, R. (1977). Granulocyte rheology: Experimental studies in an *in vitro* micro-flow system. *In* "Advances in Microcirculation" (B. M. Altura, E. Davis, and H. Harders, Eds.), Vol. 7, pp. 29–48. Karger, Basel.

CHIEN, S., SUNG, K.-L. P., SKALAK, R., USAMI, S., AND TÖZEREN, A. (1978). Theoretical and experimental studies on viscoelastic properties of erythrocyte membrane. *Biophys. J.* **24**, 463–487.

DINTENFASS, L. (1962). Thixotropy of blood and proneness to thrombus formation. *Circ. Res.* **11**, 233–239.

DRIESSEN, G. K., FISCHER, T. M., HAEST, C. W. M., INHOFFEN, W., AND SCHMID-SCHÖNBEIN, H. (1984). Flow behaviour of rigid red blood cells in the microcirculation. *Int. J. Microcirc. Clin. Exp.* **3**, 197–210.

DULING, B. R. (1978). Oxygen, metabolism and microcirculatory control. *In* "Microcirculation" (G. Kaley and B. M. Altura, Eds.), Vol. 2, pp. 401–429. University Park Press, Baltimore.

EVANS, E. A. (1983). Bending elastic modulus of red blood cell membrane derived from buckling instability in micropipet aspiration tests. *Biophys. J.* **43**, 27–30.

EVANS, E. A., AND SKALAK, R. (1980). "Mechanics and Thermodynamics of Biomembranes." CRC Press, Boca Raton, FL.

FAHRAEUS, R., AND LINDQVIST, T. (1931). The viscosity of blood in narrow capillary tubes. *Amer. J. Physiol.* **96**, 562–568.

FISCHER, T. M., HAEST, C. W. M., STÖHR-LIESEN, M., AND SCHMID-SCHÖNBEIN, H. (1981). The stress-free shape of the red blood cell membrane. *Biophys. J.* **34**, 409–422.

FITZ-GERALD, J. M. (1969). Mechanics of red-cell motion through very narrow capillaries. *Proc. R. Soc. London. B* **174**, 193–227.

GAEHTGENS, P. (1980). Flow of blood through narrow capillaries: Rheological mechanisms determining capillary hematocrit and apparent viscosity. *Biorheology* **17**, 183–189.

GAEHTGENS, P., DÜHRSSEN, C., AND ALBRECHT, K. H. (1980). Motion, deformation and interaction of blood cells and plasma during flow through narrow capillary tubes. *Blood Cells* **6**, 799–812.

GAEHTGENS, P., AND SCHMID-SCHÖNBEIN, H. (1982). Mechanisms of dynamic flow adaptation of mammalian erythrocytes. *Naturwissenschaften* **69**, 294–296.

GORCZYNSKI, R. J., KLITZMAN, B., AND DULING, B. R. (1978). Interrelations between contracting striated muscle and precapillary microvessels. *Amer. J. Physiol.* **235**, H494–504.

HONIG, C. R., ODOROFF, C. L., AND FRIERSON, J. L. (1980). Capillary recruitment in exercise: Rate, extent, uniformity, and relation to blood flow. *Amer. J. Physiol.* **238,** H31–H42.

KLITZMAN, B., DAMON, D. N., GORCZYNSKI, R. J., AND DULING, B. R. (1982). Augmented oxygen supply during striated muscle contraction in the hamster: Relative contributions of capillary recruitment, functional dilation, and reduced tissue PO2. *Circ. Res.* **51,** 711–721.

LEE, J. S., AND FUNG, Y. C. (1969). Modeling experiments of a single red blood cell moving in a capillary blood vessel. *Microvasc. Res.* **1,** 221–243.

LIGHTHILL, M. J. (1968). Pressure-forcing of tightly fitting pellets along fluid-filled elastic tubes. *J. Fluid Mech.* **34,** 113–143.

LIN, K. L., LOPEZ, L., AND HELLUMS, J. D. (1973). Blood flow in capillaries. *Microvasc. Res.* **5,** 7–19.

LINDBOM, L., AND ARFORS, K.-E. (1985). Mechanisms and site of control for variation in the number of perfused capillaries in skeletal muscle. *Int. J. Microcirc. Clin. Exp.* **4,** 19–30.

LINDBOM, L., TUMA, R. F., AND ARFORS, K.-E. (1980). Influence of oxygen on perfused capillary density and capillary red cell velocity in rabbit skeletal muscle. *Microvasc. Res.* **19,** 197–208.

LINGARD, P. (1979). Capillary pore rheology of erythrocytes. V. The glass capillary array: Effect of velocity and hematocrit in long bore tubes. *Microvasc. Res.* **17,** 272–289.

NICOLL, P. A., AND WEBB, R. L. (1955). Vascular patterns and active vasomotion as determiners of flow through minute vessels. *Angiology* **6,** 291–308.

SANDISON, J. C. (1932). Contraction of blood vessels and observations on the circulation in the transparent chamber in the rabbit's ear. *Anat. Rec.* **54,** 105–127.

SECOMB, T. W., AND GROSS, J. F. (1983). Flow of red blood cells in narrow capillaries: Role of membrane tension. *Int. J. Microcirc. Clin. Exp.* **2,** 229–240.

SECOMB, T. W., AND SKALAK, R. (1982). A two-dimensional model for capillary flow of an asymmetric cell. *Microvasc. Res.* **24,** 194–203.

SECOMB, T. W., SKALAK, R., ÖZKAYA, N., AND GROSS, J. F. (1986). Flow of axisymmetric red blood cells in narrow capillaries. *J. Fluid Mech.* **163,** 405–423.

SKALAK, R., ÖZKAYA, N., AND SECOMB, T. W. (1986). Biomechanics of capillary blood flow. *In* "Frontiers in Biomechanics" (G. W. Schmid-Schönbein, Ed.), pp. 299–313. Springer, New York.

SKALAK, R., AND TÖZEREN, H. (1980). Flow mechanics in the microcirculation. *In* "Mathematics of Microcirculation Phenomena" (J. F. Gross and A. Popel, Eds.), pp. 17–40. Raven Press, New York.

SUTERA, S. P., SESHADRI, V., CROCE, P. A., AND HOCHMUTH, R. M. (1970). Capillary blood flow. II. Deformable model cells in tube flow. *Microvasc. Res.* **2,** 420–433.

TIMOSHENKO, S. (1940). "Theory of Plates and Shells," McGraw–Hill, New York.

TÖZEREN, H., AND SKALAK, R. (1978). The steady flow of closely fitting incompressible elastic spheres in a tube. *J. Fluid Mech.* **87,** 1–16.

ZARDA, P. R., CHIEN, S., AND SKALAK, R. (1977a). Interaction of viscous incompressible fluid with an elastic body. *In* "Computational Methods for Fluid–Solid Interaction Problems" (T. Belytschko and T. L. Geers, Eds.), pp. 65–82. Amer. Soc. Mechanical Engineers, New York.

ZARDA, P. R., CHIEN, S., AND SKALAK, R. (1977b). Elastic deformations of red blood cells. *Biorheology* **10,** 211–221.